Polym. Bull. (2011) 66:377–389
DOI 10.1007/s00289-010-0346-2

ORIGINAL PAPER

SEM study of the morphology of asymmetric cellulose acetate membranes produced from recycled agro-industrial residues: sugarcane bagasse and mango seeds

Moacir Fernandes Ferreira Júnior · Elaine Angélica Ribeiro Mundim · Guimes Rodrigues Filho · Carla da Silva Meireles · Daniel Alves Cerqueira · Rosana Maria Nascimento de Assunção · Marcos Marcolin · Mara Zeni

Received: 25 January 2010 / Revised: 21 June 2010 / Accepted: 30 June 2010 /
Published online: 11 July 2010

Abstract Cellulose, obtained both from sugarcane bagasse and mango seeds, was used for synthesizing cellulose acetate in order to produce asymmetric membranes. These were compared to membranes of commercial cellulose acetate (Rhodia). All produced membranes were asymmetric, characterized by the presence of a dense skin and a porous support. Differences regarding the morphology of the surfaces as well as of the porous support can be noticed. Scanning Electron Microscopy (SEM) showed that the morphology of the superficial layer, responsible for transport, depends on the different lignin content of the starting material and also on the viscosity average molecular weight of the cellulose acetates produced from sugarcane bagasse, mango seed, and Rhodia's commercial cellulose acetate.

Keywords Cellulose acetate · Sugarcane bagasse · Mango seed · Asymmetric membrane · SEM

M. F. Ferreira Júnior · E. A. R. Mundim · G. R. Filho (✉) · C. da Silva Meireles
Instituto de Química da Universidade Federal de Uberlândia (IQ-UFU), Av. João Naves de Ávila, 2121, Cx. P. 593, Uberlândia, MG CEP 38400-902, Brazil
e-mail: guimes@ufu.br; guimes.rodriguesfilho@gmail.com

D. A. Cerqueira
Instituto de Ciências Ambientais e Desenvolvimento Sustentável da Universidade Federal da Bahia (ICADS-UFBA), Barreiras, BA, Brazil

R. M. N. de Assunção
Faculdade de Ciências Integradas do Pontal da Universidade Federal de Uberlândia (FACIP-UFU), Campus do Pontal, Ituiutaba, MG, Brazil

M. Marcolin · M. Zeni
Departamento de Física e Química, Universidade de Caxias do Sul (UCS), Caxias do Sul, RS, Brazil

Introduction

The production of cellulose derivatives using cellulose from residues such as sugarcane bagasse has been explored by the Group of Polymer Recycling of the Federal University of Uberlândia, as it can be noticed in the production of cellulose acetate [1–6] and in studies concerning the production of methylcellulose from sugarcane bagasse (SCB) [7–10].

Brazil is expected to produce 697.8 million metric tons in 2010, the world's major sugarcane production. Also, this production has been raising 1% per year and is caused by the high demand for fuel ethanol for its inner market and also for exporting. For this reason, several new mills have been assembled and the planted area is being expanded [11].

For every metric ton of sugarcane, 280 kg dry SCB is produced. This agro-industrial residue has been used for several purposes such as generating electricity, for the production of alcohol through enzymatic hydrolysis, so that SCB is becoming a byproduct of the sugar and alcohol industry [12].

Mango seed (MNG) may become another important source of cellulose in Brazil, for which there is no use up to this moment. MNG production has been increasing due to the improving in the fruit crop sector. This sector has been receiving special attention of the Brazilian development agencies and, recently, the Brazilian National Counsel of Technological and Scientific Development in partnership with the Brazilian Ministry of Science and Technology invested around US$ 1.5 million for the development of Local Productive Arrangements in the fruit crop field, which is one of the most important areas in Brazilian agriculture. Present in every Brazilian state, the fruit crop sector is a field in development, making Brazil the third major fruit producer in the world, using about 2.8 million ha to produce about 43 million metric tons of fruit, 21 million of which feed the inner market and the remaining is exported. In the city of Araguari-MG, for example, in the region of the Triângulo Mineiro, 1,300 metric tons of MNG are produced each year. The positive results reflect socially and economically, generating 5.6 million direct jobs. The improving in this sector goes through investments in technological innovation, with new genetic material and adequate producing systems.

In this sense, as SCB, MNG is an important residue that should be investigated as source for the production of cellulose derivatives. Most of the references related to mango deal with its pulp quality and characterization [13] or the use of residues produced by the industry, such as the use of residues of the juice extraction (seed and husk) for extracting bioactive compounds (enzymes, phenolic compounds, carotenoids, vitamins, pectin) [14], and the use of starch from the seed for producing glucose [15], i.e., the production of cellulose derivatives from this residue is not investigated.

Cellulose acetate is, commercially, one of the most important cellulose derivatives due to its broad range of application, such as in fibers, plastics, and production of membranes for separation processes (MSP) [16–18], which are based in different separation mechanisms as well as in the kind of utilized membrane. Asymmetric membranes are widely used in systems such as reverse osmosis, hemodialysis, and separation of organic mixtures [19–22] and consist on a top thin

layer (skin), which is dense or with small pores and is responsible for the selectivity. The skin is supported on a porous sub-layer, which provides mechanical resistance to the skin and offers low resistance to transport [23].

Therefore, the aim of this article was to investigate of the morphology of asymmetric membranes of cellulose acetate obtained from SCB and MNG, since these have not been described in the literature yet. The produced membranes had their morphologies characterized by Scanning Electron Microscopy (SEM).

Experimental

SCB purification

For cellulose extraction, 4.000 g of dry ground SCB was immersed in 100 mL of water. After 24 h, it was filtered and immersed in 100.0 mL of NaOH (0.25 M). After 18 h this mixture was vacuum filtered. The bagasse was put into a reflux with three successive portions of a mixture containing nitric acid and ethanol 1/4 (v/v), which was replaced after each hour. After the reflux, the mixture was filtered and washed with distilled water in order to remove the acid. The cellulose was dried in an oven at 105 °C for 3 h and then ground in a blender [4]. This procedure was also utilized for MNG.

MNG treatment

MNG (1.000 g), previously washed with water and dried, was immersed in NaOH 1 M for 24 h. Then, the mixture was filtered, washed with distilled water and neutralized with acetic acid 10% v/v. The material was dried in an oven at 90 °C for 3 h and stored for posterior use. In order to acetylate the mango seed it is necessary a pre-treatment of the fibers, in which 20 mL water was added to 1.000 g of the fiber and stirred for 30 min. Next, the mixture was vacuum filtered and the fibers mixed with glacial acetic acid and stirred for 30 min. Then, the acetylation reaction was carried out as described in "Production of cellulose acetate" section.

Characterization of the sugarcane bagasse and mango seeds cellulose

The materials were characterized according to their content of Klason lignin, according to Vieira et al. [9]. The molecular weight of the SCB and MNG cellulose was determined by measuring the intrinsic viscosity of dilute solutions according to NBR 7730, which is based on TAPPI test method T 230 om-08 [22]. The solvent used for dissolution of cellulose was cupriethylenediamine hydroxide solution (Cuen). From the data of intrinsic viscosity, the degree of polymerization of cellulose can be calculated according to Eq. 1:

$$\mathrm{DP}^{0.905} = 0.75\eta \tag{1}$$

where DP is the degree of polymerization and η is the intrinsic viscosity.

Production of cellulose acetate

A mixture composed of 2.000 g cellulose (from SCB or MNG) and 50 mL acetic acid was stirred for 30 min at room temperature. Then, a solution composed by 0.16 mL H_2SO_4 and 18 mL acetic acid was added to the system, which was stirred for 25 min. The mixture was filtered and 64 mL acetic anhydride was added to the filtrate. This solution was returned to the recipient containing cellulose and stirred for 30 min. After this time, the mixture stood for 14 h at room temperature. Then, this mixture was vacuum filtered to remove undissolved particles and water was added to the filtrate to stop the reaction and precipitate cellulose triacetate, which was filtered, washed with distilled water to remove acetic acid and dried at 70 °C for 2 h [1].

Next, the material was deacetylated to produce cellulose diacetate according to the following procedure.

Cellulose triacetate (2,000 g) was dissolved in 40.00 mL acetic acid. Then, a mixture composed of 1.50 mL sulfuric acid and 4.40 mL water was added to the system, which was put into reflux at 80 °C for 10 min. Next, the solution was filtered in a fritted funnel to remove insoluble particles and water was added to precipitate cellulose diacetate. The mixture was vacuum filtered and washed in order to remove acetic acid. The material was dried in oven for 2 h at 50 °C .

Cellulose acetate characterization

Fourier transformed infrared

Fourier transformed infrared (FTIR) spectra were obtained in an IR Prestige 21 (Shimadzu) FTIR spectrophotometer. The samples were prepared as tablets, using KBr (1/100 w/w). Each spectrum was recorded using 28 scans at 4 cm^{-1} resolution.

Degree of substitution

The degree of substitution (DS) was determined through an acid–base titration [24, 25], which follows.

5.00 mL NaOH (0.25 mol L^{-1}) and 5.00 mL ethanol were added to 0.1000 g cellulose diacetate. After 24 h, 10.00 mL hydrochloric acid (0.25 mol L^{-1}) was added to the system. After 30 min, the mixture was titrated using NaOH, previously standardized against potassium biphthalate using phenolphthalein as indicator. The degree of substitution was calculated according to Eq. 2.

$$\%\mathrm{GA} = \frac{[(\mathrm{Vb}_i + \mathrm{Vb}_t)\mu_\mathrm{b} - (V_\mathrm{a} \cdot \mu_\mathrm{a})]M \cdot 100}{m_\mathrm{ac}} \tag{2}$$

where %GA is the acetyl group content, Vb_i is the volume of sodium hydroxide added in the beginning of the procedure, Vb_t is the volume of sodium hydroxide spent in the titration, μ_b is the molar concentration of sodium hydroxide, V_a is the volume of hydrochloric acid added, μ_a is the molar concentration of hydrochloric acid, M is the molar weight of the acetyl groups and m_ac is the weight of the cellulose acetate sample.

Viscosity average molecular weight of cellulose acetate

Molecular weights of produced and commercial cellulose acetate were calculated from intrinsic viscosities [η] of dilute solutions, which were calculated from flux measurements of solvent and solutions in an Ostwald viscometer. The solvent used for cellulose diacetate was dichloromethane/ethanol (4/1 v/v) [26]. The viscometer was kept in a thermostated bath at 25 °C.

Relative viscosity, η_r, is calculated using Eq. 3, using flux times of solvent and solution

$$\eta_r = \frac{t}{t_0} \tag{3}$$

where t and t_0 is the solution and the solvent's flux time, respectively.

Specific viscosity, η_{sp}, is then calculated according to Eq. 4, using η_r values.

$$\eta_{sp} = \eta_r - 1 \tag{4}$$

Intrinsic viscosity, [η], is calculated according to Huggins equation (Eq. 5) [27]:

$$\frac{\eta_{sp}}{C} = [\eta] + b[\eta]^2 C \tag{5}$$

where C is the solution concentration and b is a constant.

Viscosity average molecular weight of the material is related to its intrinsic viscosity according to Mark–Houwink–Sakurada equation (Eq. 6) [27].

$$[\eta] = K(\overline{M}_v)^a \tag{6}$$

where K and a are constants related to the polymer, solvent and temperature, [η] is the intrinsic viscosity, and $\overline{M}_v$ is the viscosity average molecular weight. For the used solvent system, K is 13.9 $\times$ 10^{-3} mL g^{-1} and a is 0.834 [26].

Production of cellulose acetate membranes

The membranes were produced using the formulation described by Khulbe et al. [28] with small alterations, as follows: cellulose diacetate (15%), acetone (74%) and water (11%). The mixture was stirred for 24 h in order to dissolve completely, and then, cooled down to 4 °C. The solution was cast on a glass plate, using a casting knife with 330 μm gap at room temperature (28 °C). After 1 min, the system was immersed in a water bath at 4 °C for 2 h. The membrane was removed and then immersed into a water bath at 85 °C for 10 min. Commercial cellulose acetate (Rhodia), as well as cellulose acetate obtained from sugarcane bagasse and mango seeds were used to produce the membranes.

Scanning electron microscopy

The morphological analysis of gold-coated membrane samples (surface and cross-sections) was carried out through SEM in an Edax Phillips XL30 equipment, using

10 and 20 keV. The cross-section microscopies were obtained from membranes fractured in liquid nitrogen.

Water vapor flux

The water vapor flux through the membranes was measured using the Payne's cup technique [5]. The membrane was cut into the shape of a disk with the same diameter of the Payne's cup and had its thickness previously measured with a micrometer. Water was added to the cup and the disk was placed onto the cup's support. The system was weighed and put into a desiccator. The weight loss was measured each hour for 9 h, after which the weight loss had already reached the steady-state regimen. Water vapor flux was calculated according to Eq. 7.

$$J = \frac{\Delta m}{\Delta t} A \tag{7}$$

where J is the water vapor flux, Δm is the mass difference, Δt is the time difference, and A is the membrane area.

Diffusion of ions

For these experiments, it was used a two-compartment system separated by the studied membrane. One of the compartments was filled with deionized water, and the other with KCl solution (1×10^{-3} mol L^{-1}). A calibration curve was built by measuring the conductivity of several concentrations of KCl solutions. This curve was posteriorly used to calculate the concentrations of KCl during the diffusion experiments. From the slope of the concentration in function of time, the flux (J) through the membrane was calculated. The permeability coefficient (P) was calculated from Eq. 8.

$$P = \frac{J}{\Delta C} \tag{8}$$

where ΔC is the concentration difference between the two compartments.

The diffusion coefficients (D) through the membranes were calculated using the Eq. 9.

$$D = Pd \tag{9}$$

where d is the membrane thickness.

Gas permeability

Tests were carried out in a stainless steel cell with permeation area of 8.04 cm^2, using N_2 as permeation gas at 1 kg cm^{-2} pressure. Permeated gas was collected and measured in a graduated cylinder filled with water. Measurements were taken at regular intervals in order to observe the flux repeatability. Gas permeability was calculated according to Eq. 10:

$$P_{N_2} = \frac{Vl}{AtP} \tag{10}$$

where V is the gas volume (cm^3), l is the thickness (cm), A is the area (cm^2), t is the time (s), and P is the pressure (cmHg).

Results and discussion

Determination of Klason lignin and molecular weight of cellulose from Sugarcane Bagasse and mango seeds

SCB presented 23.8 and 3.84% of Klason lignin before and after the cellulose extraction, respectively [9]. MNG presented 26.6 and 24.3% of Klason lignin before and after treatment with NaOH 1 mol L^{-1}, respectively. In spite of the lignin content remained nearly the same, this step is important since NaOH solution causes cellulose mercerization, resulting in greater accessibility to the fibers of mango seed during the acetylation reaction. Purified mango seed presented 4.5% Klason lignin and posterior results showed that the lignin content has influence on the membrane morphology.

The morphology of the membrane can be also influenced by the molecular weight of cellulose acetate. Cellulose acetate was produced from cellulose extracted from SCB and MNG and the values of molecular weight obtained by viscosity measurements were 107,000 g mol^{-1} for sugarcane bagasse cellulose and 91,000 g mol^{-1} for mango seed cellulose. For agroindustrial wastes, the molecular weights are relatively close and indicate that there is no significant difference between the two original materials in relation to molecular weight.

Cellulose acetate characterization

Figure 1 shows typical FTIR spectra of cellulose acetate produced from SCB and MNG.

Absorption bands in 1756 cm^{-1} (carbonyl groups of ester), 1237 cm^{-1} (C–C–O stretching of acetate), 1047 cm^{-1} (C–O stretching) characterizes these materials as cellulose acetate [29, 30], which present distinct degrees of substitution (DS). DS is the average value of cellulosic glucosidic hydroxyl groups replaced by acetyl groups. Commercial cellulose acetate presents DS of 2.45, as stated by the manufacturer, was kindly provided by Rhodia-Santo André/SP, Brazil, and was used as reference. DS of cellulose acetate produced from SCB and MNG were 2.37 and 2.49, respectively. Therefore, both are classified as cellulose diacetate [31]. The Viscosity average molecular weight $\overline{M}_v$ calculated for the materials was 46000, 27600, and 16,700 g mol^{-1} for cellulose diacetates from Rhodia (RHO-CA), mango seed (MNG-CA) and sugarcane bagasse (SCB-CA), respectively. As the MNG has a higher amount of lignin in relation to SCB cellulose, the reaction of acetylation and deacetylation leads to subsequent hydrolysis of the lignin initially present, which partially protects cellulose. As the sample of mango seed contains the highest lignin

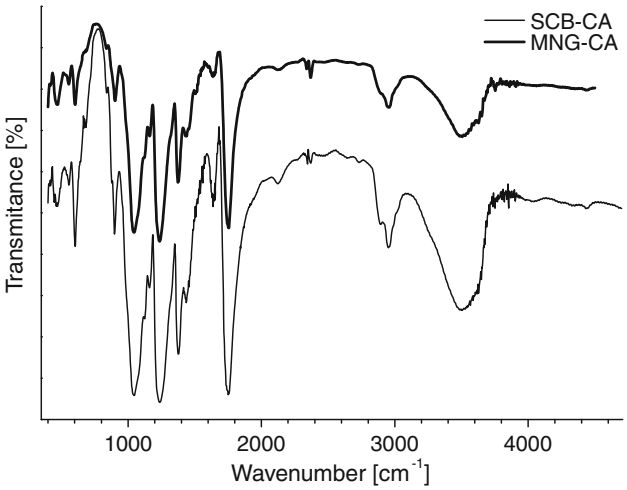

Fig. 1 FTIR spectra of cellulose acetate produced from sugarcane bagasse (SCB) and mango seed (MNG)

content among the samples, it is observed for this sample a decrease in molecular weight by about 69.0%. Although this value is high, the observed decrease is less pronounced than that observed for the cellulose acetate produced from SCB cellulose (about 84.0%). These differences in molecular weight of the materials result in different morphologies of the membranes structures, as it will be seen later.

Membrane characterization

Scanning electron microscopy

Membrane SEM photos (cross-sections and surfaces in contact with air) of the materials are shown in Figs. 2 and 3, respectively. Figure 2 shows that all membranes are asymmetric, since there is a superficial layer with higher density onto the porous layer. However, the morphological differences on the membranes can also be observed in the porous support formation, where a porous structure with open cells is observed for RHO-CA.

During the phase inversion process the separation is induced in solution by changes in composition or temperature, which makes the solution thermodynamically unstable. Evaporation of the solvent causes an increase in the concentration of polymer in solution until the precipitation occurs due to the presence of non-solvent. The formation of a thin film begins in the interface polymer solution/air. The high polymer concentration may lead to the formation of skin due to viscous effects promoted by the phenomena of coalescence and gelation. The mass transfer between the polymer solution and the bath promotes separation of liquid–liquid phase, giving rise to a polymer-rich phase and to a polymer-lean phase. The high concentration of the polymer-rich phase leads to a decrease in the rate of the mass transport system, leading to the formation of the porous support from

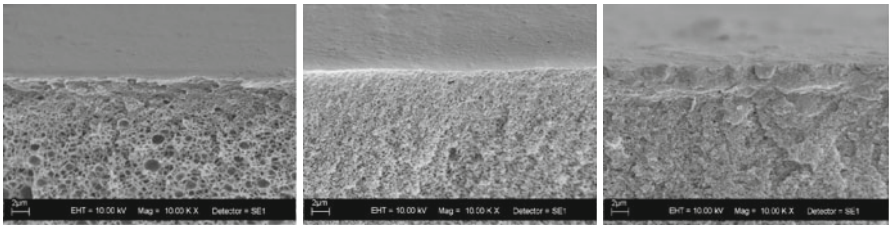

RHO-CA (a) MNG-CA (b) SCB-CA (c)

Fig. 2 Cross-sections of the membranes **a** RHO-CA, **b** MNG-CA, and **c** SCB-CA (×10,000)

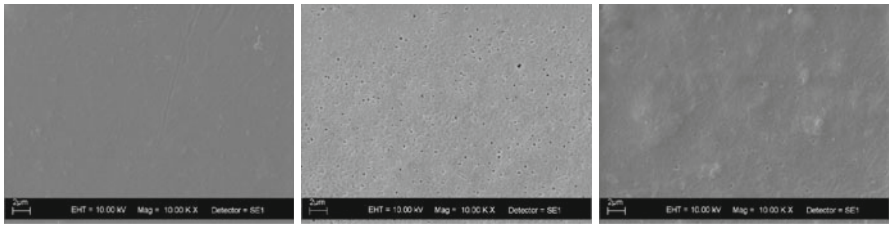

RHO-CA (a) MNG-CA (b) SCB-CA (c)

Fig. 3 SEM of the surfaces in contact with air **a** RHO-CA, **b** MNG-CA, and **c** SCB-CA (×10,000)

the polymer-lean solution. Several factors influence the different morphologies that can be produced, the types of solvent and non-solvent, use of additives in polymer solution and the coagulation bath composition. The porous support shown in Fig. 2b, c denote areas with high polymer densities. For this systems the parameters such as polymer concentration, non-solvent concentration, solvent evaporation time, coagulation bath temperature, and post treatment bath, used in the preparation of the membranes were the same for all materials. Considering this aspect, the membrane morphologies can be related to differences in the molecular weight and lignin content of cellulose acetate.

Whereas the polymer solutions were produced with the same percentage of polymer, for cellulose acetate produced with major molecular weight (RHO) the polymer solution shows high viscosity. That favors the formation of a dense surface film from the phenomena of gelation, being the quality of the film formed directly related to the viscosity of the solution. This viscous polymer-rich solution causes the decrease of mass transport between the coagulation bath, the polymer-lean solution and substrate, leading to formation of a porous open cell structure from the polymer-lean solution and the formation of an integral dense skin as can be seen in Figs. 2a and 3a, respectively. Therefore, RHO-CA membrane is expected to have the skin with highest density, followed by MNG-CA and then by SCB-CA. However, MNG-CA membrane presents pores throughout its skin extension and the skin of SCB-CA membrane presents regions of higher density than MNG-CA membranes (Fig. 3).

In this case, the lignin content need to be considered because it has significant influence on the membrane morphology. Lignin fragments can modify the membrane morphology by reducing the solubility of the polymer/lignin system,

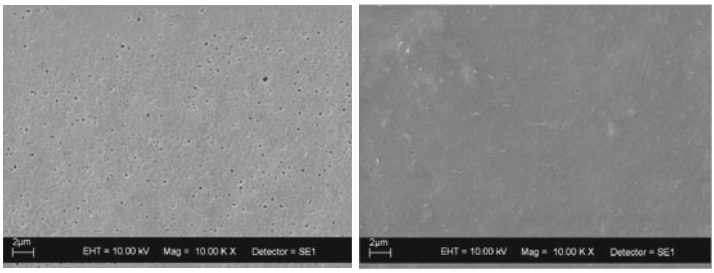

MNG-CA (a) MNG-CA1 (b)

Fig. 4 Surfaces in contact with air **a** MNG-CA and **b** MNG-CA1 (×10,000)

Table 1 Water vapor flux, gas permeability (N_2) and ion coefficient diffusion for the produced membranes

Materials	Normalized flux J L ($g\ s^{-1}\ cm^{-2}\ \mu m$)	Gas permeability ($cm\ s^{-1}\ cm\ Hg^{-1}$)	Ion coefficient diffusion ($cm^2\ s^{-1}$)
RHO-CA	1.06×10^{-4}	0.01×10^{-12}	9.27×10^{-7}
MNG-CA1	0.80×10^{-4}	4.80×10^{-12}	1.43×10^{-7}
SCB-CA	1.25×10^{-4}	10.40×10^{-12}	0.55×10^{-7}
MNG-CA	1.60×10^{-4}	76.10×10^{-12}	28.00×10^{-7}

leading to the precipitation of these components during the skin formation. Lignin is present in cellulose and remains in the cellulose acetate after the acetylation [31] reaction and was determined by Klason lignin method, which the lignin content for the MNG-CA was 5.17% and for the SCB-CA was 3.70%. In this case, these lignin fragments interact with the polymer and can affect the interaction between the polymer chains, producing low-density regions. That is confirmed in Fig. 4, which shows the SEM photo of a membrane of cellulose acetate produced from purified mango seeds (MNG-CA1), for which the raw material went through the same purification process than sugarcane bagasse, having its lignin content in cellulose acetate reduced to about 3.20%. The morphology of the top layer (skin) of this material is similar to the morphology of SCB-CA membrane, confirming that the lignin content affects significantly the final morphology of the membranes.

Measurements of water vapor flux, permeability to gas (N_2) and ion diffusion

Values of water vapor flux, gas permeability (N_2), and ion coefficient diffusion for the produced membranes are presented in Table 1.

The step that determines the transport speed occurs most of the times through the superior layer (skin). However, it is possible that other mechanisms, such as the flux resistance of the porous sub-structure, contribute to the transport through the membrane [32]. According to Table 1, the water vapor flux values indicate differences in morphology that were demonstrated also by gas permeability measurements, where the permeability values are smaller for RHO-CA membrane,

followed by values of the MNG-CA1, of the SCB-CA, and posteriorly by the values of the membrane of MNG-CA, corroborating with the previously observed morphologies where skin density of the membranes follows this same order. Therefore, the water vapor flux and gas permeability were controlled mainly by the superficial layer of the membranes. On the other hand, the coefficient of ion diffusion showed that the transport through the membranes is controlled also by the porous sub-structure. The value of the coefficient of ion diffusion presented for membrane SCB-CA was small when compared to the other materials. This result is corroborated by the morphology presented in Fig. 2, where the structure for this membrane is less asymmetric and presents a morphology that seems uniform throughout the thickness, what hampers the ion diffusion in this membrane.

Conclusion

The degree of substitution of cellulose acetate produced from cellulose of purified sugarcane bagasse and treated mango seed present values of 2.49 ± 0.03 and 2.37 ± 0.01, respectively, characterizing these materials as cellulose diacetates. Viscometric average molecular weight ($\overline{M}_v$) of cellulose diacetate produced from sugarcane bagasse and mango seed were 16,700 and 27,600 g mol^{-1}, respectively, and Rhodia's cellulose diacetate $\overline{M}_v$ was 46,000 g mol^{-1}. These differences in molecular weight, as well as the different lignin contents, resulted in distinct membrane structures, specially on the morphology of the superficial layer (skin) which have an important role on the transport through the membranes, as it was seen in the results of water vapor flux and gas diffusion. On the other hand, on the ion diffusion experiments the porous substructure influences the transport through the membranes where the SCB-CA membrane has a substructure with higher polymer density, presenting a lower value for the coefficient of ion diffusion.

Acknowledgments The authors acknowledge to CNPq for project Casadinho UFU/UFG/UFMS (620181/2006-0), to CAPES for the access to "Portal Periódicos", to Finep/Sebrae for project 0535/07 ref 3119/06. Meireles thanks CAPES for her PhD scholarship, Ribeiro thanks FAPEMIG for the scholarships related to projects PIBIC A-025/2008 e EX—APQ-00466-08.

References

1. Cerqueira DA, Rodrigues Filho G, Meireles CD (2007) Optimization of sugarcane bagasse cellulose acetylation. Carbohydr Polym 69(3):579–582
2. Cerqueira DA, Rodrigues G, Assuncao RMN (2006) A new value for the heat of fusion of a perfect crystal of cellulose acetate. Polym Bull 56(4–5):475–484
3. Meireles CDS, Rodrigues Filho G, de Assuncao RMN, Zeni M, Mello K (2007) Blend compatibility of waste materials—cellulose acetate (from sugarcane bagasse) with polystyrene (from plastic cups): diffusion of water, FTIR, DSC, TGA, and SEM study. J Appl Polym Sci 104(2):909–914
4. Rodrigues Filho G, da Cruz SF, Pasquini D, Cerqueira DA, Prado VD, de Assuncao RMN (2000) Water flux through cellulose triacetate films produced from heterogeneous acetylation of sugar cane bagasse. J Membr Sci 177(1–2):225–231
5. Rodrigues Filho G, da Silva RC, Meireles CD, da Assuncao RMN, Otaguro H (2005) Water flux through blends from waste materials: cellulose acetate (from sugar cane bagasse) with polystyrene (from plastic cups). J Appl Polym Sci 96(2):516–522

6. Rodrigues Filho G, Toledo LC, Cerqueira DA, de Assuncao RMN, Meireles CD, Otaguro H, Rogero SO, Lugao AB (2007) Water flux, DSC, and cytotoxicity characterization of membranes of cellulose acetate produced from sugar cane bagasse, using PEG 600. Polym Bull 59(1):73–81
7. Rodrigues Filho G, de Assuncao RMN, Vieira JG, Meireles CD, Cerqueira DA, Barud HD, Ribeiro SJL, Messaddeq Y (2007) Characterization of methylcellulose produced from sugar cane bagasse cellulose: crystallinity and thermal properties. Polym Degrad Stab 92(2):205–210
8. Vieira RGP, Meireles CS, de Assunção RMN, Filho GR (2004) In: Production and characterization of methylcellulose from sugar cane bagasse, 5th International symposium on natural polymers and composites; 8th Brazilian symposium on the chemistry of lignins and the other wood components. São Pedro-SP, Brazil, pp 1–3
9. Vieira RGP, Rodrigues Filho G, de Assuncao RMN, Meireles CDS, Vieira JG, de Oliveira GS (2007) Synthesis and characterization of methylcellulose from sugar cane bagasse cellulose. Carbohydr Polym 67(2):182–189
10. Viera RGP (2004) Síntese e caracterização da metilcelulose a partir da metilação heterogênea do bagaço de cana-de-açúcar. Universidade Federal de Uberlândia, Uberlândia, MG, Brazil
11. IBGE (2010) http://www.ibge.gov.br/home/estatistica/indicadores/agropecuaria/lspa/lspa_201005_5.shtm. Accessed 28 May 2010
12. Copersucar (2010) http://www.copersucar.com.br/institucional/por/academia/cana_acucar.asp. Accessed 28 May 2010
13. Olle D, Lozano YF, Brillouet JM (1996) Isolation and characterization of soluble polysaccharides and insoluble cell wall material of the pulp from four mango (*Mangifera indica* L) cultivars. J Agric Food Chem 44(9):2658–2662
14. Ajila CM, Bhat SG, Rao UJSP (2007) Valuable components of raw and ripe peels from two Indian mango varieties. Food Chem 102(4):1006–1011
15. Velan M, Krishnan MRV, Lakshmanan CM (1995) Conversion of mango kernel starch to glucose syrups by enzymatic-hydrolysis. Bioprocess Eng 12(6):323–326
16. Chou WL, Yu DG, Yang MC, Jou CH (2007) Effect of molecular weight and concentration of PEG additives on morphology and permeation performance of cellulose acetate hollow fibers. Sep Purif Technol 57(2):209–219
17. Meireles CD (2007) Síntese e caracterização de membranas de acetato de celulose, obtido do bagaço de cana-de-açúcar, e blendas de acetato de celulose com poliestireno de copos plásticos descartados. Universidade Federal de Uberlândia, Uberlândia, MG, Brazil
18. Sossna M, Hollas M, Schaper J, Scheper T (2007) Structural development of asymmetric cellulose acetate microfiltration membranes prepared by a single-layer dry-casting method. J Membr Sci 289(1–2):7–14
19. Delanaye P, Lambermont B, Dogne JM, Dubois B, Ghuysen A, Janssen N, Desaive T, Kolh P, D'Orio V, Krzesinski JM (2006) Confirmation of high cytokine clearance by hemofiltration with a cellulose triacetate membrane with large pores: an in vivo study. Int J Artif Organs 29(10):944–948
20. Duarte AP, Bordado JC, Cidade MT (2007) Cellulose acetate reverse osmosis membranes: optimization of preparation parameters. J Appl Polym Sci 103(1):134–139
21. Ismail AF, Hassan AR (2004) The deduction of fine structural details of asymmetric nanofiltration membranes using theoretical models. J Membr Sci 231(1–2):25–36
22. Kalocheretis P, Vlamis I, Belesi C, Makriniotou I, Zerbala S, Savidou E, Zorbas S, Arvanitis N, Iatrou C (2006) Residual blood loss in single use dialyzers: effect of different membranes and flux. Int J Artif Organs 29(3):286–292
23. Kesting RE (1985) Synthetic polymeric membranes: a structural perspective, 2nd edn. Wiley, New York
24. Puleo AC, Paul DR, Kelley SS (1989) The effect of degree of acetylation on gas sorption and transport behavior in cellulose-acetate. J Membr Sci 47(3):301–332
25. Rodrigues Filho G, Monteiro DS, Meireles CD, de Assuncao RMN, Cerqueira DA, Barud HS, Ribeiro SJL, Messadeq Y (2008) Synthesis and characterization of cellulose acetate produced from recycled newspaper. Carbohydr Polym 73(1):74–82
26. Knaus S, Bauer-Heim B (2003) Synthesis and properties of anionic cellulose ethers: influence of functional groups and molecular weight on flowability of concrete. Carbohydr Polym 53(4):383–394
27. Sperling LH (1992) Introduction to physical polymer science, 2nd edn. Wiley, New York
28. Khulbe KC, Matsuura T, Lamarche G, Lamarche AM, Choi C, Noh SH (2001) Study of the structure of asymmetric cellulose acetate membranes for reverse osmosis using electron spin resonance (ESR) method. Polymer 42(15):6479–6484

29. He JX, Zhang M, Cui SZ, Wang SY (2009) High-quality cellulose triacetate prepared from bamboo dissolving pulp. J Appl Polym Sci 113(1):456–465
30. Mark JE (1999) Polymer data handbook. Oxford University Press, Oxford
31. Sassi JF, Chanzy H (1995) Ultrastructural aspects of the acetylation of cellulose. Cellulose 2(2): 111–127
32. Mulder M (1997) Basic principles of membranes technology, 2nd edn. Edition Academic Publishers, The Netherlands